INTERACTIONS OF VOLTAGE-SENSING DYES WITH MEMBRANES

II. Spectrophotometric and Electrical Correlates of Cyanine-Dye Adsorption to Membranes

S. Krasne, *Department of Physiology, Ahmanson Neurobiology Laboratory, and Molecular Biology Institute, University of California, Los Angeles, California 90024 U.S.A.*

ABSTRACT The adsorption to bilayer membranes of the thiadicarbocyanine dyes, $diSC_n(5)$, has been studied as a function of the membrane's surface-charge density, the aqueous ionic strength, and the length (n) of the hydrocarbon side chain of the dye. "Probe" measurements in planar bilayers, microelectrophoresis of liposomes, and measurement of changes in dye absorbance and fluorescence in liposomes were used to study dye adsorption to membranes. These measurements indicated that the membrane:water partition coefficient for the dye monomer increases with the length of the hydrocarbon side chain. However, the formation of large aggregates in the aqueous phase also increases with increasing chain length and ionic strength so that the actual dye adsorbing to the membrane goes through a maximum at high but not at low ionic strengths. More dye adsorbs to negatively charged than neutral membranes. Membrane-bound dye spectra were easily resolved in negatively charged liposomes where it was observed that these dyes could exist as monomers, dimers, and large aggregates. For $diSC_1(5)$ a spectral peak was observed at low but not high ionic strengths (i.e. the conditions in which this dye appears to form voltage-gated channels) corresponding to small aggregates which appeared to adsorb to the membrane. Finally, the adsorption of these dyes to membranes results in more positive electrostatic potentials composed primarily of dye-induced "boundary" potentials and somewhat less of "double-layer" potentials.

INTRODUCTION

In the previous paper (Krasne, 1980; referred to here as paper I), it was shown that cyanine dyes alter the intrinsic permeability properties of phospholipid bilayer membranes. The mechanisms by which dye-induced permeability changes were brought about were shown to depend upon dye structure, dye concentration, membrane surface-charge density, and ionic strength. The present paper attempts to examine the manner in which dye adsorption to membranes and concomitant dye-induced electrostatic potential changes depend upon these same factors.

MATERIALS AND METHODS

Materials

The materials were the same as those described in the previous paper with the following additions: Egg phosphatidylcholine (PC)[1] was obtained from Lipid Products (England); dioleoyl lecithin (diol PC) was

[1] *Abbreviations used in this paper:* diol PC, dioleoyl lecithin; m.a.r., monomer absorbance ratio; PC, phosphatidylcholine; PE, phosphatidylethanolamine; PS, phosphatidylserine.

obtained from Avanti Biochemicals Inc. (Birmingham, Ala.); nonactin was a gift from Barbara Stearn of E.R. Squibb & Sons (Princeton, N.J.); and monactin was a gift (to George Eisenman) from Dr. Hans Bickel (of CIBA). Chemicals were used without further purification. Aliquots of concentrated ethanolic solutions of nonactin and monactin were added to the aqueous phases in the planar bilayer experiments, the final concentration of ethanol from this source never exceeding 1%.

Methods

In addition to the methods described in the previous paper, the following techniques were employed:

LIPOSOME FORMATION Single-lamellar egg PC liposomes were prepared according to the method of Batzri and Korn (1973). 1:1 PC/phosphatidylserine liposomes (PC/PS) were prepared by evaporating (under a stream of N_2) $CHCl_3$/EtOH solutions of these lipids in a test tube, shaking them in the desired (N_2-purged) aqueous solution, and sonicating for 5–10 min (Branson sonifier W350, Branson Sonic Power Co., Danbury, Conn.) until the light scattering produced was minimized (i.e., no longer decreased with further sonication). Titanium particles were removed by centrifugation. All liposomes were checked for excessive oxidation by comparing the absorbance at 215 and 230 nm (Klein, 1970) and the lipid concentrations (determined spectroscopically) were set equal to 2 mM (or ~1.8 mg/ml). The absorbance of all solutions was checked at 450 nm and the range of variation among solutions was found to be less than a factor of 2, which was considered tolerable. Although some fraction of the resulting liposomes were undoubtedly multilamellar, controls indicate that the present dyes penetrate the membrane fast enough that after ~15 min the spectra depend only upon the concentration of lipid and not on the amount of sonication (and ergo the number of lamellae). Multilamellar vesicles for the electrophoresis experiments were formed by the method of Bangham et al. (1974).

SPECTROSCOPIC MEASUREMENTS Absorbance measurements were made using an Hitachi model 60 double-beam, UV/visible spectrophotometer (Hitachi Ltd., Tokyo, Japan), and fluorescence measurements were made using an Aminco-Bowman spectrophotofluorometer (with excitation and emission slits set for 14 nm (American Instrument Co., Inc., Silver Springs, Md.)). Both photometers were equipped with Hamamatsu 446 photomultiplier tubes to enhance their sensitivities at the longer (visible) wavelengths. The spectra were uncorrected except for base-line subtraction. In the case of the absorbance spectra, the reference solution was the same as the sample solution except for the presence of dye in the sample cuvette; the absorbance of the sample never exceeded 0.2 A at any measured wavelength. Solutions were stirred continuously during all spectroscopic measurements.

A major problem was encountered because of the adsorption of dye to the cuvette (Sims et al., 1974; Hladky and Rink, 1976). The amount of dye adsorbed to the cuvette at any time could be determined by totally emptying the cuvette of solution by suction, adding EtOH, and measuring the resulting absorbance spectrum after it had stabilized. In the 15-min period after addition of dye to give a 10^{-6} M solution, approximately 10–35% of the dye had adsorbed to the cuvette. The disappearance of dye from solution continued for at least 2 hr; however after about 15–30 min (depending on the dye) the rate of change of absorbance with time was sufficiently slow (1%/ min) that significant distortion of the spectra did not occur, and spectra were measured after this time.

The spectroscopy experiments illustrated in Figs. 4, 5, 12, and 13 were carried out by first adding dye (to 10^{-6} M) to the aqueous solution in the sample cuvette and waiting until the rate of change of absorbance at 645 nm (i.e. the aqueous monomer peak) was <1%/min. The absorbance spectrum and subsequently the fluorescence emission and excitation spectra were then scanned. The first aliquot of liposomes was added to the sample and reference cuvettes and absorbance monitored at 645 nm until again the rate of change of absorbance was <1%/min. Absorbance and fluorescence spectra were measured again. Subsequent aliquots of liposomes were added and the above procedure repeated until the final liposome addition was made (usually yielding a total of 0.237 mg/ml lipid) and the spectra measured. The solutions were then aspirated from the sample and reference cuvettes, EtOH was added, and the absorbance spectrum (after a steady state was obtained) measured to determine the amount of dye adsorbed to the cuvette. If the particular combination of dye and liposomes present in a cuvette was such that little adsorption of dye to the liposomes took place, then the total amount of dye in the solution

and liposome membranes decreased slightly during the course of the experiment as a result of continued dye adsorption to the cuvette; by the end of such an experiment, up to half the total dye was bound to the wall of the cuvette. If the dye adsorbed strongly to the liposomes, by the end of the experiment no dye was found to remain on the walls of the cuvette. Thus the variation in the dye concentration in the aqueous solution between the measurement of the first and last spectra or between experiments on different dyes and/or different liposomes can be as much as a factor of 2. For purposes of the present paper, therefore, only the trends in the dye spectral properties are examined.

In the measurements of Hladky and Rink (1976) on erythrocytes, they used a combination of short stirring periods, preequilibration of the cuvette with the dye and measurement of the dye bound to the cuvette after each single addition of erythrocytes. This method yields much more quantitative results than the ones used here. However, to complete the number of measurements necessary for the present paper, this method would have required a sufficiently heroic effort that the increase in quantitation would not have justified the increase in effort. In addition, we have found that even using a preequilibration technique, tremendous variation exists among the dyes, as well as for any one dye at different ionic strengths, in the concentration of dye remaining in the aqueous solution, and in contrast to the observations of Hladky and Rink (1976), different amounts of dye were found to desorb from the glass depending upon whether the dye, liposome and ionic strengths were such as to yield strong or weak adsorption of dye to the liposomes.

The one case in which the exact dye concentrations associated with the spectra were calculated was for the spectra in Fig. 4 A and B. For these figures, dye was added to the cuvette to 10^{-6} M and stirred for 10 min. The dye was then left unstirred for an additional 5 min and the absorbance spectrum measured. The solutions were aspirated from the sample and reference cuvettes, 3 ml of EtOH was added, stirred, and the spectrum measured after a steady state of absorbance was reached. Depending on the dye and the aqueous solution, between 6.5×10^{-7} M and 7.5×10^{-7} M dye had remained in the aqueous solution. To compare the aqueous spectra, therefore, the observed spectrum (after base-line subtraction) was multiplied by the factor $7 \times 10^{-7}\ \mathrm{M}/C_{dye}$ where C_{dye} was the aqueous dye concentration remaining at the time of the absorbance measurements. Thus, one assumption underlying the spectra of Fig. 4 A and B is that a significant change in the relative proportions of the various aggregates for a given dye does not occur over the range 6.5×10^{-7}M–7.5×10^{-7} M. This assumption seems reasonable.

MICROELECTROPHORESIS MEASUREMENTS Electrokinetic mobilities were measured with a Rank Brothers Mark I microelectrophoresis apparatus (Bottisham, Cambridge, England). Care was taken to focus at the stationary layer (Henry, 1938) and to monitor for electrode polarization.

RESULTS

Cyanine Dyes Alter the Membrane's Electrostatic Potential

To determine whether dyes alter the membrane's electrostatic potential, one can investigate whether, and to what degree, dyes alter the conductances induced by lipid-soluble ions and/or ion-carrier complexes (McLaughlin et al., 1971; Szabo et al., 1972; McLaughlin, 1977). (The "electrostatic potential" of the membrane refers here to the electrical potential difference between the midpoint of the membrane [in the transverse direction] and the bulk aqueous phase in the absence of a voltage difference between the two aqueous phases.) In such experiments, the conductance-inducing species serve as "probes" of the membrane's electrostatic potential. In principle, one would like to use oppositely charged probes to determine whether the conductance alteration observed is due to an effect of the dyes on the electrostatic potential of the membrane surface (in which case the conductances induced by oppositely charged probes would be altered in opposite directions) or on the standard chemical potential

of the membrane interior (e.g. due to changes in viscosity, dielectric constant, etc., in which case the probe-induced conductances would be altered in the same direction, regardless of their charge). I have investigated the effects of the cyanines, $diSC_n(5)$, on conductances mediated by the cation carriers nonactin and monactin as well as the anionic permeant species I_5^- (iodine/iodide), $CCCP^-$ (carbonyl cyanide-*m*-chlorophenyl hydrazone), and tetraphenylborate. In all cases the cyanines formed complexes with the anionic species, to the point that these species could not be used as probes. Therefore an alternative experiment was performed in which the effects of the oppositely charged oxonol and cyanine dyes on the nactin-induced conductances were investigated. The results of such experiments are shown in Fig. 1. (The oxonol-induced conductances were always much lower than the nonactin-K^+-mediated conductances.) Because the oxonols used have structures which are analogous to those of the cyanines, but they are oppositely charged (Bashford et al., 1979), one would expect that the magnitude of their adsorption to neutral bilayers would be similar to that of the cyanines and that the consequences of such adsorption might also be similar except that any electrostatic potentials produced would be of opposite sign. Clearly, as seen in Fig. 1, the oxonols enhance the nactin-mediated conductances whereas cyanines depress them suggesting that major effect induced by both of these classes of dyes is an alteration in the electrostatic potential of the membrane. (Spectroscopic studies indicate that the initial decrease in nonactin-mediated conductance observed in the presence of OxVII is due to a small degree of complexation between the nonactin-K^+ complex and this dye. This effect is slighly present for OxVI and not at all for OxV.)

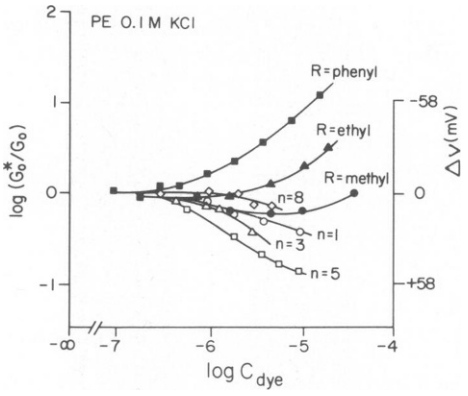

FIGURE 1 Effects of oppositely charged dyes on nactin-mediated membrane conductances. The left-hand ordinate is the log of the ratio of nactin-mediated conductances in PE bilayers in the presence (G_d^*) and absence (G_0) of dye, the log of dye concentration being specified by the abscissa. The right-hand ordinate is the calculated dye-induced change in the membrane's electrostatic potential. The solid symbols represent nonactin-K^+-mediated conductances in the presence of the (negatively charged) oxonols Ox VII (●), Ox VI (▲), and Ox V (■). The open symbols represent monactin-K^+-mediated conductances in the presence of the (positively charged) cyanines $diSC_1(5)$ (○), $diSC_3(5)$ (△), $diSC_5(5)$ (□), and $diSC_8(5)$ (◇). All measurements were made in 0.1 M KCl and 2×10^{-6} M nonactin or 10^{-6} M monactin, and for the oxonols, the solution was buffered at pH 7 with *N*-2-hydroxyethyl piperazine-*N*-2-ethane sulfonic acid. In all cases the conductances were significantly larger than those observed in the absence of nonactin or monactin. Note that the negatively charged oxonols generally enhance the nactin-K^+-mediated conductance whereas the positively charged dyes suppress it. (The initial suppression observed in the presence of Ox VII is due to some degree of complexation of the negatively charged oxonols with the nonaction-K^+ complex, as discussed in the text.)

Cyanine-induced Alteration in the Membrane's Electrostatic Potential Are a Function of Membrane Surface-Charge Density, Ionic Strength, and Dye Chain Length

Two obvious expectations for cyanines are (*a*) that they would be more concentrated on the surface of negatively charged than neutral membranes (because, being positively charged, they would be more strongly attracted towards a negatively charged surface than a neutral one), and (*b*) that the longer the dye's hydrocarbon chain length (at least up to the point that the side chain length approaches that of the lipid), the more readily it would stick to the membrane (both because of greater induced-dipole interactions with the hydrocarbon chains of the membrane lipids and because of greater disruption of water-water interactions). If these dyes alter the membrane's electrostatic potential by altering the membrane's surface-charge density (and thus the "double-layer" potential), there is a third expectation, which is less obvious intuitively but which can be deduced from Gouy-Chapman diffuse double-layer theory. This is that an increase in ionic strength should decrease the surface-potential change induced by these dyes (although the actual dye concentration on the membrane, and thus the surface-charge density, should increase). These expectations are treated quantitatively, for charged species which are reversibly adsorbed to membrane surfaces, by McLaughlin and Harary (1976).

The data in Fig. 2 illustrate that these three expected behaviors are generally observed for $diSC_1$ (5), $diSC_3$ (5), and $diSC_5$ (5) but not for $diSC_8$ (5). This figure is composed of four subfigures, each of which is analogous to Fig. 1 and illustrates the effect of increasing the

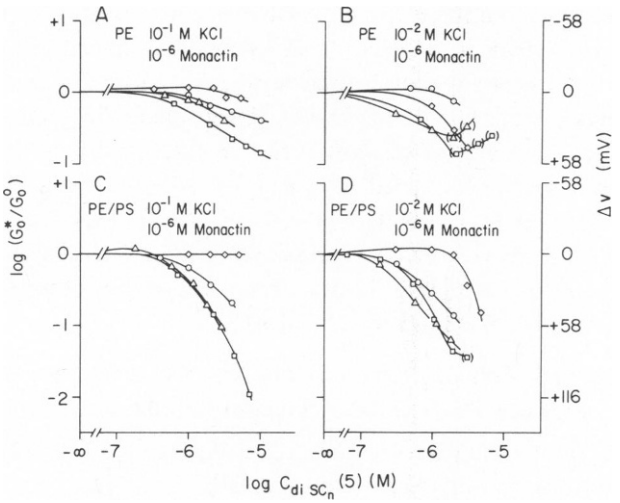

FIGURE 2 Effects of dye structure, ionic strength, and membrane surface-charge density on the alteration of monactin-K^+-mediated conductances by cyanine dyes. In all subfigures, the ordinates, abscissa, and symbols for each dye are the same as in Fig. 1, the concentration of monactin is 10^{-6} M, and the ionic strength is equal to the KCl concentration. (A) PE bilayers in 10^{-1} M KCl; $G_0 = 8\ (\pm 0.76) \times 10^{-5}\ \Omega^{-1}\ cm^{-2}$. (B) PE bilayers in 10^{-2} M KCl. The data points in parentheses reflect dye-induced conductances as well as those due to monactin-K^+ (cf. conductance values for dyes in Fig. 1 of paper I) since the initial carrier-mediated conductance values at this KCl concentration and in this lipid were quite low; $G_0 = 1.4\ (\pm 0.48) \times 10^{-5}\ \Omega^{-1}\ cm^{-2}$. (C) PE/PS bilayers in 10^{-1} M KCl; $G_0 = 5\ (\pm 2.7) \times 10^{-4}\ \Omega^{-1}\ cm^{-2}$. (D) PE/PS bilayers in 10^{-2} M KCl; $G_0 = 1.57\ (\pm 0.86) \times 10^{-4}\ \Omega^{-1}\ cm^{-2}$.

cyanine dye concentration on monactin-K^+-mediated bilayer conductance. Two subfigures (Fig. 2 A and B) are for neutral phosphatidyl ethandamine (PE) bilayers and two (Fig 2 C and D) for negatively charged bilayers (PE/PS); similarly two (Fig. 2 A and C) are for 0.1 M ionic strength and two (Fig. 2 B and D) for 0.01 M ionic strength. For $diSC_n(5)$, the dye-induced electrostatic potential change increases as n goes from 1 to 5 and, for these three dyes, is larger in negatively charged than neutral membranes and at lower than at higher ionic strength. The electrostatic potential alterations induced by $diSC_8(5)$ tend to be smaller than those for the other dyes, and are slightly larger in neutral than negatively charged membranes, these observations being opposite to those expected (although the ionic strength effect is as predicted).

The data of Fig. 2 reflect an additional anomaly in the behavior of these dyes which is not expected from simple Gouy-Chapman diffuse double-layer theory (or the more general treatment encompassed by the Stern equation; see McLaughlin and Harary, [1976] and that is that for several of the dyes the electostatic potential changes too steeply with increasing dye concentrations (cf. especially $diSC_5(5)$ and $diSC_8(5)$ at 10^{-2} M ionic strength and $diSC_3(5)$ and $diSC_5(5)$ in PE/PS bilayers at 0.1 M ionic strength). The maximum predicted value for neutral membranes for $\Delta\log(G_0^*/G_0)/\Delta\log C_{Dye}$ is 2/3 for the case in which the dye adsorbs to the membrane surface as a singly charged monomer (Andersen et al., 1978), whereas for membranes having one negative charge per two lipid molecules, it can be shown by the same procedure (unpublished observation) that $\Delta\log(G_0^*/G_0)/\Delta\log C_{Dye} \leq 1$ for a positive, singly charged monomer. The steeper dependences observed in Fig. 2 are predicted (unpublished result) if charged dimers and/or trimers are the predominant adsorbed dye species, especially (for neutral membranes) when these aggregates also include anions (i.e., in the present case, Cl^-). Andersen et al. (1978; also Tsien, 1978) have also demonstrated that such steep dependences of surface potential on the concentration of adsorbed species can arise from discrete charge effects. This latter effect is likely to be of significant magnitude, however, only when the adsorbed charges are sufficiently buried in the membrane that the electrostatic potentials they produce are not "screened" by ions in the aqueous phase, thereby resulting in a sizable "boundary potential" (Andersen et al., 1978). To examine the origins of the anomalous electrostatic-potential behaviors observed for these dyes as well as whether they do indeed produce "boundary potentials" rather than screenable double-layer potentials, I examined the zeta potentials produced by these dyes.

The Electrostatic Potentials Produced by the Dyes Are Accounted for Largely by Their Production of Boundary Potentials

The zeta potentials, ζ, of neutral (diol PC) and negatively charged (diol PC/PS 1:1) liposomes in the presence and absence of dyes were calculated from the measured values of the electrophoretic mobilities, u, by the Helmholtz-Smoluchowski equation:

$$\zeta = u\epsilon_r\epsilon_0/\eta \tag{1}$$

where η is the viscosity of the aqueous phase, ϵ_r is the dielectric constant and ϵ_0 is the permittivity of free space. The differences between the zeta potentials measured in the presence and absence of dye for a given liposome and aqueous composition are plotted in Fig. 3. Comparing the zeta potentials induced by the dyes with the total electrostatic potentials deduced from conductance measurements (Fig. 2, right-hand ordinate), it can be seen that the

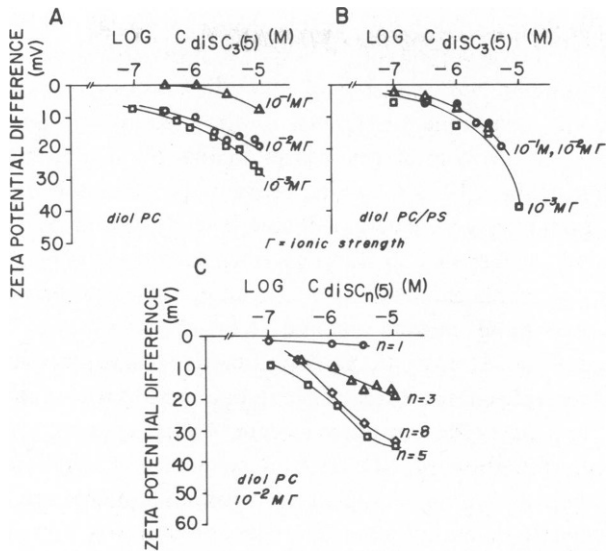

FIGURE 3 Zeta potentials produced by cyanine dyes. The ordinate is the difference between the zeta potential measured in the presence and absence of the dye concentration designated by the abscissa. The temperature was 25°C. The standard deviations of the experimental points (n = 10) are less than the diameter of the symbols. The zeta potentials of diol PC liposomes in the absence of dye were −4 (±1), −0.8 (±0.85), and 0 (< ±1) mV for 10^{-3}M, 10^{-2} M and 10^{-1} M ionic strengths, respectively. The zeta potentials of diol PC/PS (1:1) liposomes in the absence of dye were −57.6 (±8), −44.5 (±5.7) and −27 (±1.4) mV at 10^{-3}M, 10^{-2}M, and 10^{-1} M ionic strengths, respectively. (A) Zeta potential differences induced by $diSC_3(5)$ in neutral (diol PC) liposomes. The lipid concentration was 10 μg/ml. Symbols denote 10^{-1} M (Δ), 10^{-2} M (○), and 10^{-3} M (□) ionic strengths. (B) Zeta potential differences induced by $diSC_3(5)$ in negatively charged (diol PC/PS, 1:1) liposomes. The lipid concentration was 10 μg/ml. Symbols are as in A. (C) Zeta potential differences induced by cyanine dyes in neutral (diol PC) liposomes at 10^{-2} M ionic strength. The lipid concentration was 10 μg/ml. Symbols denote $diSC_1(5)$ (○), $diSC_3(5)$ (Δ), $diSC_5(5)$ (□), and $diSC_8(5)$ (◇).

zeta potentials are significantly smaller than the total electrostatic potentials. For example, comparing data from Fig. 3 A with that from Fig. 2 A and B, the zeta potential induced by 2×10^{-6} M $diSC_3(5)$ in neutral liposomes is 2 mV at 10^{-1} M ionic strength (Γ) and 14 mV at 10^{-2} MΓ; the electrostatic potentials inferred from the bilayer conductance measurements for comparable conditions were 13 and 36 mV, respectively. An analogous comparison for the same conditions but comparing negatively charged liposomes (Fig. 3 B) and bilayers (Fig. 2 C and D) yields zeta potential differences of 12 mV for both ionic strengths but electrostatic potentials differences of 41 and 70 mV for 10^{-1} M and 10^{-2} M ionic strengths, respectively. That the same general discrepancy exists for all of the dyes can be seen by comparing the data of Fig. 3 C with that of Fig. 2 B. Thus, not all of the electrostatic potential difference induced by the dyes in membranes is "screenable."

Some discrepancy is expected between the membrane's double-layer potential and the zeta potential measured at high ionic strength since the plane of shear is about 2 Å from the membrane surface whereas at high ionic strength, the double-layer potential lies much closer to the membrane surface. At 10^{-3} M ionic strength this discrepancy would be negligible, and at 10^{-1} M ionic strength, a zeta potential of 20 mV would predict a double-layer potential of

30 mV whereas a zeta potential of 60 mV would predict a double-layer potential of 80 mV (Eisenberg et al., 1979). These corrections are still not sufficient to account for the observed discrepancies. A reasonable interpretation of this observation is that the dye is buried sufficiently far into the membrane that much of the electrostatic potential difference it produces falls off between the plane of dye adsorption and the membrane surface and is thus not screenable (Andersen et al., 1978). An alternative interpretation is that the dye sits at the membrane surface producing a screenable double-layer potential as well as altering the orientation of the lipid headgroups so as to produce a "non-screenable" dipole potential change. These two alternatives cannot now be distinguished. The discrepancy between the total electrostatic potential and the zeta potential does support the possibility, however, that the steep dependences of the electrostatic potentials on dye concentration observed in several cases could be due to discrete charge effects from dyes adsorbed within the bilayer (similar to the effects suggested previously for tetraphenylborate; Andersen et al., 1978).

The alternative interpretation of the steep dependence of electrostatic potentials on dye concentration is that the dye forms aggregates within the membrane phases. To examine the anomalous electrostatic-potential behaviors induced by $diSC_8(5)$ as well as to determine whether these dyes do indeed form aggregates in the membrane phase, I examined the spectral properties for these dyes.

The Influence of Membrane Surface Charge, Ionic Strength, and Dye Structure on the Adsorption of Dyes to Membranes Parallels Their Effects in Modulating Dye-induced Electrostatic Potentials

Absorbance spectra for the dyes in 10^{-3} M and 10^{-1} M ionic strength solutions are illustrated in Fig. 4 A and B, respectively, along with designations of the wavelengths associated with monomer, dimer, H-aggregate (i.e. small aggregates) and J-aggregate (i.e. large aggregates) peaks (Waggoner et al., 1977; West and Pearce, 1965). Certain striking differences among the dyes can be observed as a function of increasing chain length and ionic strength. First considering $diSC_3(5)$ and $diSC_5(5)$, it can be seen that the predominant peak for these dyes is that for the dye monomer although $diSC_5(5)$ shows a larger dimer peak and smaller monomer peak than does $diSC_3(5)$. For $diSC_1(5)$, there is a significant monomer peak, although less than for $diSC_3(5)$, and in addition there is a peak in the wavelength region for H-aggregates which is significant at 10^{-3} M but much smaller at 10^{-1} M ionic strength. Finally, for $diSC_8(5)$, a very broad spectrum is observed, spanning the range of wavelengths from J-aggregates to H-aggregates. At 10^{-3} M ionic strength, a small peak can be observed at the monomer wavelength but not at 10^{-1} M ionic strength. Whereas a negligible degree of light scattering is observed in fluorescence measurements on aqueous solutions of the shorter-chained dyes, significant scattering is observed in those of $diSC_8(5)$. Because the spectra for these dyes in ethanol are virtually identical to each other, the data of Fig. 4 suggest not only that these dyes form aggregates in the aqueous phase but that the particular aggregates observed are a function of the dye structure and the ionic strength of the aqueous phase.[2]

---

[2]These sorts of observations are not new. Waggoner et al. (1977) showed for much higher concentrations of $diSC_2(5)$ (i.e. 10^{-5} M), that dye aggregation is much greater in 0.1 M than in distilled water and similar observations had been made and characterized previously for a number of dyes (see, for example, Kay et al., 1964). To my knowledge, no one has reported a peak in the H-aggregate region which decreases with increasing ionic strength, such as that observed for $diSC_1(5)$.

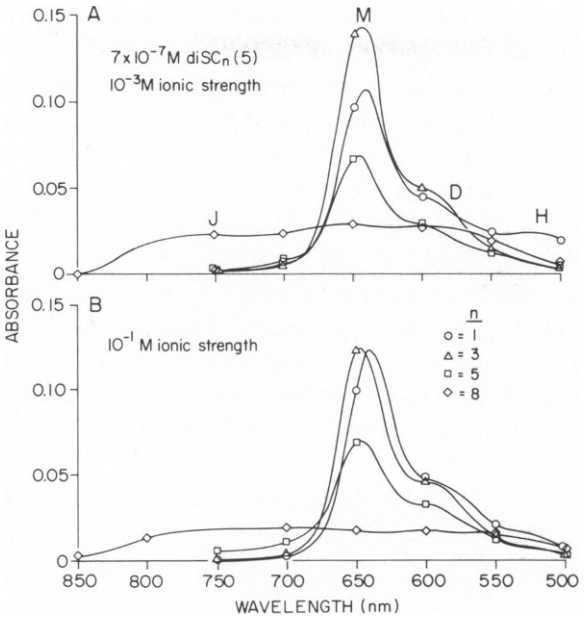

FIGURE 4 The effects of dye structure and ionic strength on the state of aggregation of cyanine dyes in the aqueous phase. In both subfigures, the ordinate is absorbance and the abscissa is wavelength. Spectra were recorded 15 min after adding the indicated dye to 10^{-6} M in either 5×10^{-4} M NaCl + 5×10^{-4} M KCl (A) or 5×10^{-2} M NaCl + 5×10^{-2} M KCl (B). Because of dye adsorption to the cuvette, the amount of dye remaining in solution at this time was $\sim 7 \times 10^{-7}$ M and the spectra were normalized to this concentration (see text for details). Symbols have been inserted into the spectra for purposes of identification only. The designations of aggregates in A inidcate the approximate wavelengths at which the major peaks are observed for each of these dye aggregates (Waggoner et al., 1977; West and Pearce, 1965). Note that the absorbance spectrum for the dye monomer has a shoulder at approximately the same wavelength as the peak due to the dimer.

TABLE I
ABSORBANCE RATIOS AT DYE-AGGREGATE WAVELENGTHS

Dye	Ionic strength	Absorbance ratios*		
		$A_{\lambda_D}/A_{\lambda_M}$	$A_{\lambda_H}/A_{\lambda_M}$	$A_{\lambda_J}/A_{\lambda_M}$
	M			
$DiSC_1$ (5)	10^{-3}	0.31	0.24	0
	10^{-1}	0.31	0.12	0
$DiSC_3$ (5)	10^{-3}	0.28	0.05	0
	10^{-1}	0.30	0.06	0
$DiSC_5$ (5)	10^{-3}	0.33	0.11	0.02
	10^{-1}	0.37	0.11	0.09
$DiSC_8$ (5)	10^{-3}	0.95	0.36	0.74
	10^{-1}	0.96	0.64	1.07

*Absorbance ratios were calculated from the data of Figs. 4 A and B. λ_M, λ_D, λ_H, and λ_J are the wavelengths associated with the monomer, dimer, H-aggregate, and J-aggregate peaks (or bands), respectively (Fig. 4 A). For $diSC_3$ (5), $diSC_5$ (5), and $diSC_8$ (5), the following values were used: λ_M = 648 nm, λ_D = 580 nm, λ_H = 525 nm, and λ_J = 750 nm. For $diSC_1$ (5), the spectrum appears to be shifted approximately 5 nm to shorter wavelengths (for a clear example, Fig. 4 B) so that the values of λ's used for this dye were 5 nm smaller than those for the other three dyes.

Table I allows a slightly more quantitative comparison among the dyes by listing the ratios of absorbance at wavelengths corresponding to the dimer, H-aggregate, and J-aggregate relative to that at the wavelength corresponding to the monomer.

Absorbance spectra for each of the dyes in 10^{-3} M and 10^{-1} M ionic strength solutions and in the presence of various concentrations of PC or PC/PS liposomes have been measured. An example of such measurements is shown for $diSC_5(5)$ in the Appendix. Most of the conclusions which can be drawn from these spectra can be inferred from the representative spectra in Figs. 5 and 6. Fig. 5 A–D illustrate the spectra observed for $diSC_1(5)$, $diSC_3(5)$, $diSC_5(5)$, and $diSC_8(5)$, respectively, in the presence of 14.8 and 237 μg/ml PC liposomes at 10^{-3} M (filled symbols) and 10^{-1} M (open symbols) ionic strength whereas Fig. 6 A–D are the analogous spectra for the dyes in 1.48 and 14.8 μg/ml PC/PS liposomes. In each figure, the dye spectra in the aqueous phase are shown for purposes of comparison. Although it is difficult to make quantitative comparisons among these data, as discussed in the Methods, certain trends are clear.

First of all, a number of additional peaks are observed in the presence of liposomes. The dye monomer spectrum in the membrane is at ~15-nm longer wavelength than the aqueous

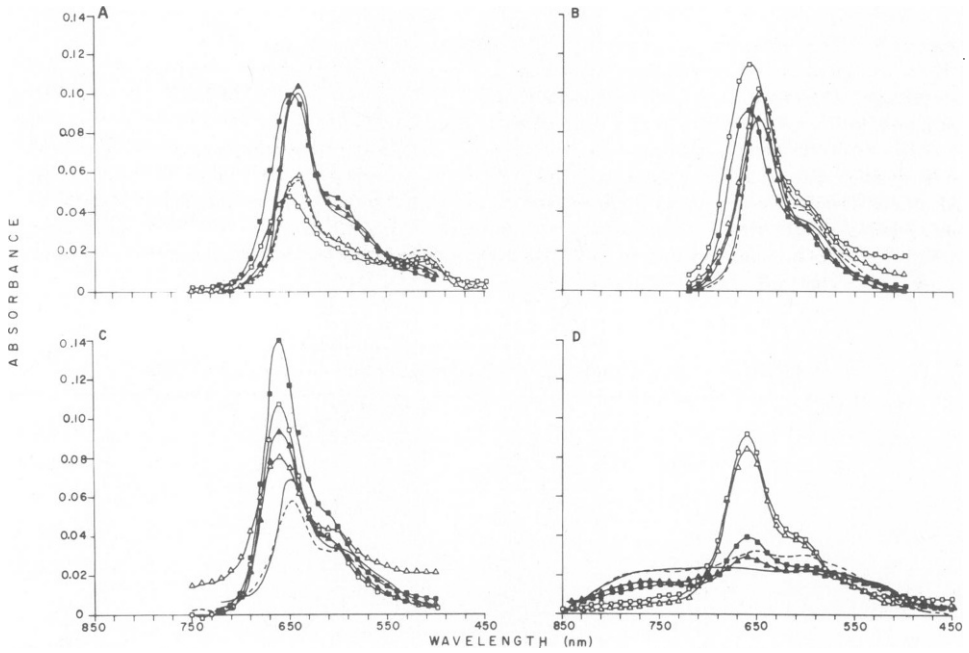

FIGURE 5 Absorbance spectra for cyanine dyes in the presence of neutral, PC liposomes. The spectra in Figs. 4 and 5 were obtained as continuous curves, and the symbols have been inserted for purposes of identification. The filled symbols in each subfigure identify spectra in 10^{-1} M ionic strength solutions whereas the open symbols identify spectra in 10^{-3} M ionic strength solutions. In addition, spectra designated by triangles were obtained in the presence of 14.8 μg/ml PC whereas those designated by squares were obtained in the presence of 237 μg/ml PC. The solid and broken curves without symbols are the spectra obtained for each dye in the 10^{-1} M and 10^{-3} M aqueous solutions, respectively, before the addition of liposomes. Subfigures A–D are spectra for $diSC_1(5)$, $diSC_3(5)$, $diSC_5(5)$, and $diSC_8(5)$, respectively.

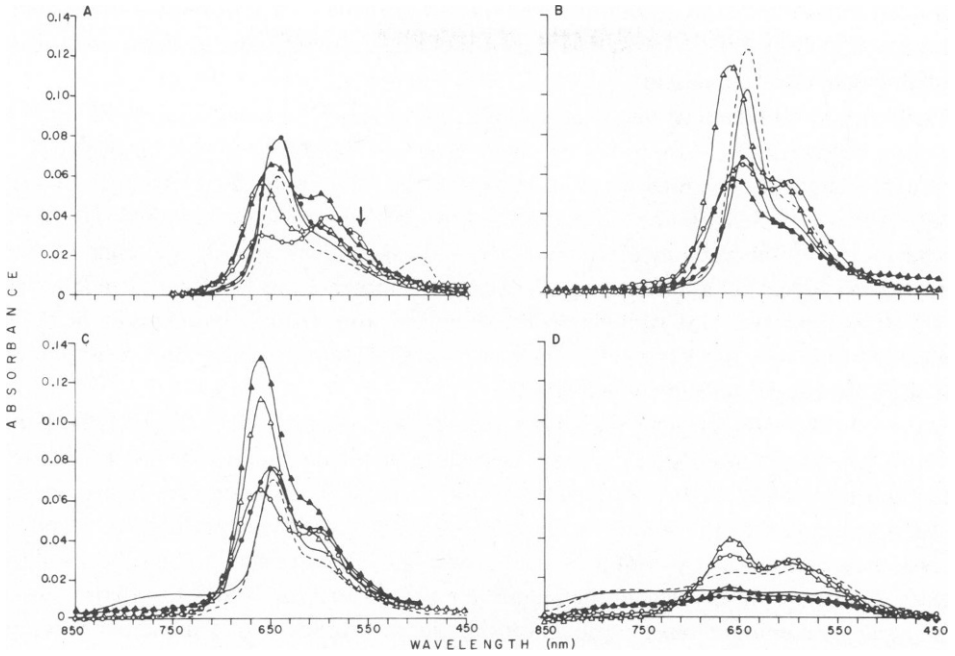

FIGURE 6 Absorbance spectra for cyanine dyes in the presence of negatively charged PC/PS liposomes. The filled symbols in each subfigure identify spectra in 10^{-1} M ionic strength solutions whereas the open symbols identify spectra in 10^{-3} M ionic strength solutions. In addition, the spectra designated by circles were obtained in the presence of 1.48 μg/ml PC/PS whereas those designated by triangles were obtained in the presence of 14.8 μg/ml PC/PS (cf, triangles in Fig. 5). The solid and broken curves without symbols are the spectra obtained for each dye in the 10^{-1} and 10^{-3} M aqueous solutions, respectively, before the addition of liposomes. Subfigures A–D are spectra for diSC$_1$(5), diSC$_3$(5), diSC$_5$(5), and diSC$_8$(5), respectively.

monomer; similarly a peak is observed for several of the dyes (e.g. diSC$_1$(5) in PC/PS liposomes) at about 10-nm longer wavelength than the aqueous dimer. These peaks represent the membrane-bound monomer and dimer, respectively (Waggoner et al., 1977). In the case of diSC$_1$(5), an additional peak is observed in 10^{-3} M ionic strength for low concentrations of PC/PS at about 30–50-nm longer wavelength than that for aqueous H-aggregates (see the arrow and open circles in Fig. 6 A) whereas for diSC$_3$(5) and diSC$_5$(5) at 10^{-3} M ionic strength the spectra are elevated in both the long and short wavelength regions upon addition of PC liposomes, this elevation decreasing at high liposome concentrations.

The peak observed for diSC$_1$(5) may correspond to small aggregates (e.g., H-aggregates) in the membrane phase and appears to occur under the same conditions (i.e. low but not high ionic strength) as those in which this dye appears to form "voltage-gated channels" (see paper I) in the membrane. It is possible that the peaks observed for diSC$_1$(5) in the region of 500–520 nm in the aqueous phase and 530–550 nm in the presence of PC/PS are due to some contaminant or isomer in this dye preparation, as may be the conductance behaviors seen for this dye. I have made similar, but less extreme, observations for both the spectral and conductance behaviors of diSC$_2$(5) under the same conditions, and no anomalous peaks are observed for these dyes in EtOH, which may argue slightly in favor of thinking that these

observations relate to the dye structure. The shift in the short-wavelength peak observed upon addition of PC/PS argues against this peak simply reflecting some absorbance due to these dyes being bound to the cuvette.

The elevations observed at low ionic strength for $diSC_3(5)$ and $diSC_5(5)$ in PC liposomes may also represent the formation of some type of membrane-bound aggregates (e.g., J-aggregates and/or H-aggregates) or may simply be due to different light-scattering properties between the liposomes with absorbed dye, in the sample cuvette, and those without adsorbed dye, in the reference cuvette. The only argument against the light-scattering interpretation is that no additional light scattering is observed in the fluorescence measurements (beyond that seen, for example, by these concentrations of PC liposomes in the presence of $diSC_1(5)$ or no dye at all), whereas such scattering should be reasonably easily discerned given the absorbance elevation which is seen.

Several trends in the influences of dye structure, membrane surface charge, and aqueous ionic strength on partitioning of dye into the membrane phase can also be observed from the spectra in Figs. 5 and 6 as well as the data of Figs. 7 and 8. These latter two figures represent an attempt to quantify the trends in the dye absorbance spectra of which Fig. 5 and 6 are representative examples, and require some explanation. Because the monomer peak shifts as these dyes go from the aqueous to the membrane phase, the ratio of the absorbance observed at the aqueous monomer wavelength to that at the membrane-bound monomer wavelength serves as an indication of the amount of dye monomer in the aqueous vs. membrane phase. For convenience I have termed this ratio the "monomer absorbance ratio" or m.a.r.. It allows comparisons among dyes whose absolute levels of absorbance may differ because of variations in the amount of dye present in the aqueous phase at the time of the measurement (due to adsorption to the cuvette). A more accurate measure could be obtained if an isosbestic point were observed for this membrane/aqueous phase partitioning; however because of the many states of the dye in each phase, no such point is observed. Unfortunately, the formation of certain types of aggregates in the aqueous phase (i.e. dimers and J-aggregates, which have secondary and primary peaks, respectively, at wavelengths near that of the membrane-bound monomer; see West and Pearce, 1965) also decreases the m.a.r.; because these particular types of aqueous aggregates increase with increasing dye chain length (Table I), the m.a.r. for the dyes in the aqueous phase, designated $(m.a.r.)_a$, decreases with increasing chain length, as is illustrated by the open circles in Fig. 6. A limiting value of the m.a.r. could also be calculated for the pure monomer species of each of the dyes in the membrane phase (this limiting value being designated $[m.a.r.]_m$) since for each of the dyes a condition of lipid composition and ionic strength was found for which all, or virtually all, of the dye was adsorbed to the membrane as monomers (i.e., no further change in spectrum was observed with increasing liposome concentration). For $diSC_5(5)$ the $(m.a.r.)_m$ could be observed for both PC and PC/PS liposomes at 10^{-3} M and 10^{-1} M ionic strengths; because for this dye, the $(m.a.r.)_m$ (and the limiting spectrum in general), appears to be independent of ionic strength or membrane composition, it is assumed to be independent for the other dyes as well. The filled circles in Fig. 7 illustrate that the $(m.a.r)_m$ for the membrane-bound dye changes only slightly as a function of dye structure, increasing with increasing chain length.

To indicate the degree of partitioning of dye between the aqueous and membrane phase, the "fractional m.a.r.," which equals $[(m.a.r.) - (m.a.r.)_m]/[(m.a.r.)_a - (m.a.r.)_m]$, is plotted as

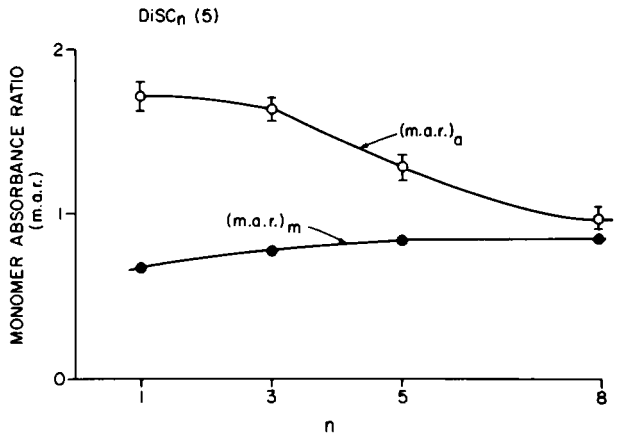

FIGURE 7 Dye monomer absorbance ratios (m.a.r.) in the aqueous and lipid phases. The ordinate is the m.a.r., which is defined for each dye as the ratio of absorbance observed at the wavelength corresponding to the aqueous dye monomer absorbance maximum to that observed at the wavelength corresponding to the absorbance maximum for the dye monomer in the lipid phase. The abscissa designates the dye, the value of n corresponding to the number of carbons in the dye's hydrocarbon side chains. Open circles are the mean data values, designated $(\text{m.a.r.})_a$, for dye added to the aqueous phases to 10^{-6} M (the actual aqueous concentrations being closer to 7×10^{-7} M at the time at which the measurements were made, see text), and the closed circles are data values, designated $(\text{m.a.r.})_m$, for the case in which the dye is totally in the membrane phase and the spectrum no longer changes with further additions of liposomes. For the aqueous phase data, the bars indicate the range of data observed in 10^{-3} M and 10^{-1} M ionic strengths and the decrease in the $(\text{m.a.r.})_a$ with increasing n is due to increased dye aggregation in the aqueous phase. Data were calculated from spectra such as those of Fig. 12 A–D.

a function of the logarithm of liposome concentration (for PC and PC/PS liposomes at 10^{-1} M and 10^{-3} M ionic strengths) for $diSC_1(5)$, $diSC_3(5)$, $diSC_5(5)$, and $diSC_8(5)$ in Fig. 7 A–D, respectively. A value of 1 for this fraction normally indicates that all of the dye is in the aqueous phase (one exception to this being discussed below), whereas a value of 0 corresponds to all of the dye being in the form of monomers in the membrane phase.

The behavior of this fractional m.a.r. parallels what one observes qualitatively in the spectra of Figs. 5 and 6, as well as Fig. 12 and the remaining unpublished spectra, with the exception of the behavior of $diSC_1(5)$ in the presence of small concentrations (i.e. <5.9 μg/ml) of PC/PS liposomes at 10^{-3} M ionic strength. Thus, for $diSC_1(5)$, $diSC_3(5)$, and $diSC_5(5)$, one can conclude that (a) increasing dye chain length increases the membrane-/aqueous-phase partition coefficient; (b) increasing the negative surface charge on the membrane increases the dye's adsorption to the membrane; and (c) increasing ionic strength decreases dye adsorption to negatively charged liposomes and increases slightly its adsorption to neutral liposomes (except for $diSC_1[5]$). In the case of $diSC_8(5)$ the behaviors are quite different. Thus, this dye appears to adsorb, strongly to liposomes at 10^{-3} M ionic strength but negligibly to liposomes at 10^{-1} M ionic strength, and to the extent that a significant difference can be inferred, it seems to adsorb more strongly to neutral than negatively charged liposomes. The former observation for $diSC_8(5)$ appears likely to be correlated with the fact that no aqueous monomers are observed at 10^{-1} M ionic strength; the apparently greater adsorption to PC than PC/PS liposomes is not explained by any obvious features of the system. In the case of

$diSC_1(5)$ in PC/PS liposomes at 10^{-3} M ionic strength, I have observed that even for the smallest addition of liposomes (0.148 μg/ml), this dye adsorbs significantly to the membrane. However, it appears that for very low PC/PS concentrations, the membrane-bound dye is all in the form of (postulated) H-aggregates so that no change is observed in the ratio of the aqueous to membrane-bound monomer even though a significant fraction of dye is in the membrane.

Comparisons of Fig. 8 with the raw absorbance and fluorescence data indicate that the steep decrease in the fractional m.a.r. observed initially with increasing lipid concentration correlates with the decrease of dye in the aqueous phase and increase in the membrane phase, whereas the less steep change frequently observed at higher liposome concentrations (especially in PC/PS) reflects a change in the state of the dye (i.e., decreased aggregation) within the membrane phase itself, no dye fluorescence being observed in this region which would correspond to the presence of dye in the aqueous phase. Indeed for several of the dyes, there were concentrations of PC/PS liposomes for which no fluorescence signal at all could be observed despite the fact that an absorbance signal corresponding to membrane-bound monomers was clearly visible (see, for example, Fig. 13 of the Appendix). These liposome concentrations correspond to those at which the inflections are observed (in going from the steep to the more gradual changes in the fractional m.a.r. with increasing lipid) in the data of Fig. 8. A likely explanation for this fluorescence behavior, as well as for the shift observed in the fluorescence maximum to shorter wavelengths as additional aliquots of PC/PS are added, is that the dye monomers are so concentrated in the membrane that the fluorescence emitted

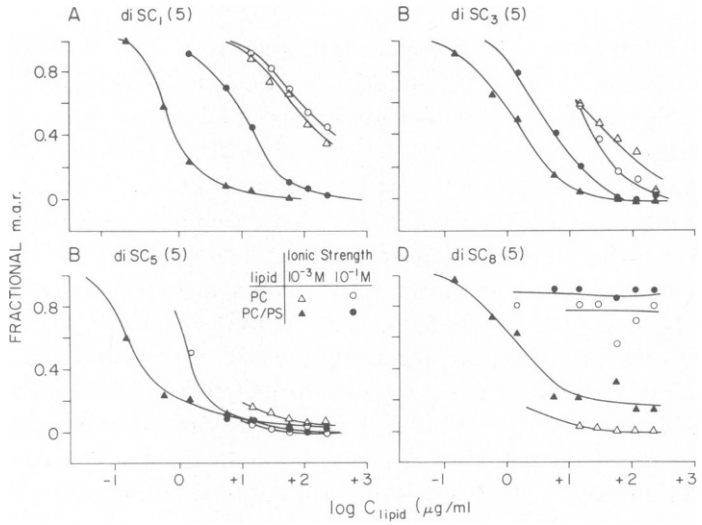

FIGURE 8 Influence of dye structure, membrane composition, and ionic strength on the partitioning of cyanine dyes between the aqueous and membrane phases. The ordinate is the "fractional m.a.r.", given by $[\text{m.a.r.} - (\text{m.a.r.})_m]/[(\text{m.a.r.})_a - (\text{m.a.r.})_m]$, observed after addition of the liposomes, the concentration of lipid in the cuvette being indicated on the abscissa. A "fractional m.a.r." equal to 1 indicates that all of the dye is in the aqueous phase whereas one equal to zero indicates that all of the dye is in the membrane phase. The data of subfigures A–D were calculated from spectra such as those in Fig. 12 A–D and are for $diSC_1(5)$, $diSC_3(5)$, $diSC_5(5)$, and $diSC_8(5)$, respectively.

by one dye monomer is absorbed by neighboring, nonfluorescent aggregates, and/or Forster energy transfer is occurring between fluorescent monomers and nonfluorescent aggregates. For all of the dyes (except $diSC_8(5)$ at 0.1 M ionic strength), aggregates in the membrane phase are observed in the presence of the smaller and intermediated concentrations of PC/PS.

Interestingly, the trends in the data of Fig. 8 as a function of dye structure and lipid composition correspond to the conclusions which can be inferred from the dye-induced electrostatic potential data of Fig. 2. Namely, as dye chain length is increased from $n = 1$ to $n = 5$, more dye adsorbs to the membrane, whereas for $n = 8$, less dye adsorbs to the membrane (except in PC at 10^{-3} M ionic strength) and for $n = 1$, 3, and 5, more dye adsorbs to negatively charged than neutral membranes whereas the reverse is true for $n = 8$. Comparisons of the effects of ionic strength would require conversion of the electrostatic potential data to surface charge densities which in turn requires some assumption as to the way to view the origins of the electrostatic potential effects (e.g., "smeared" surface charge effects, discrete charge effects, boundary potentials, etc.). The evidence thus far, however, suggests that the electrostatic potentials are composed in large part from boundary potentials and that either discrete-charge effects or dye aggregation in the membrane phase could give rise to the steep dependences of these potentials on dye concentration. (To compare the liposome and bilayer measurements, one must know whether dye dissolves in the bilayer-membrane torus. Little or no change in the spectra are observed upon adding bulk membrane-forming PE or PE/PS solutions to aqueous $diSC_3(5)$ solution. Thus the dye concentrations [at least for $diSC_3(5)$] in the planar bilayers correspond to those observed at lipid concentrations even lower than the lowest [i.e. 0.148 mg/ml] for which spectra were measured.)

Dye-induced Alterations in Membrane Electrostatic Potentials Show Little Voltage Dependence

The results cited above suggest that these dyes adsorb to the membrane, thereby altering its electrostatic potential. These dyes are thought to act as voltage sensors via a redistribution mechanism, with alterations in transmembrane voltage changing the dye distribution either between the membrane and aqueous phases or between the aqueous phases either side of the membrane (Waggoner, 1976; Cohen and Salzberg, 1978; Hladky and Rink, 1976). It is, therefore, of some interest to see whether such voltage-induced dye redistribution can be sensed by "probe" measurements. Fig. 9 illustrates the effects of these dyes on monactin-K^+ (or, for a few measurements, nonactin-K^+)-mediated conductance-voltage relationships. The solid curves in the subfigures indicate the "normalized" conductance-voltage relationship of monactin-K^+ in the absence of dye, and the data points indicate the relationships observed in the presence of the dyes. Clearly the data points in all cases lie close to, or on, the curve in each subfigure, indicating that little or no perturbation is produced by these dyes in the nactin-mediated conductance-voltage relationship. Small perturbations are seen in certain cases, however, the most clear-cut of which is that illustrated in Fig. 9 D for $diSC_8(5)$ at 10^{-2} M ionic strength in PE/PS bilayers (cf., open and filled triangles). Clearly both the data for high frequency (15 mV/s) and low frequency (2.5 mV/s) voltage ramps are similar; however, a definite difference is observed between them. Similar time dependences were observed in PE bilayers at 10^{-2} M ionic strength as well.

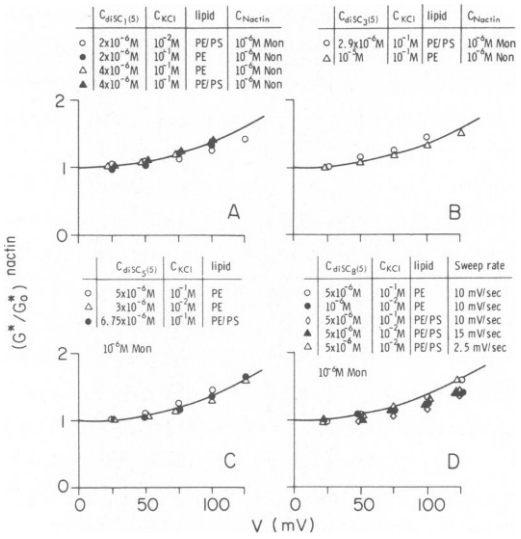

FIGURE 9 Nactin-K^+-mediated conductance-voltage behaviors in the presence of cyanine dyes. In each subfigure, the ordinated is the "normalized" conductance (i.e., the conductance divided by that observed in the limit of zero current) observed at the voltage indicated by the abscissa. Except where indicated otherwise, data represent conductances resulting from application of a 10-mV/s voltage ramp. The solid curve in each subfigure is the normalized conductance-voltage behavior induced by nonactin-K^+ or monactin-K^+ (both being the same) in PE or PE/PS membranes in the absence of dyes. Subfigures A–D are for $diSC_1(5)$, $diSC_3(5)$, $diSC_5(5)$, and $diSC_8(5)$, respectively, and the particular dye concentration, lipid concentration, ion carrier, and, where appropriate, sweep rate corresponding to each symbol is indicated in the subfigure.

DISCUSSION

The electrostatic potential induced by a given concentration of dye goes through a maximum as the length of the hydrocarbon side chain on the dye is increased, with $n=3$ and 5 producing the largest potentials; the electrostatic potentials produced by $diSC_8(5)$ are much larger at 10^{-2} M than at 10^{-1} M ionic strength. An additional aspect of the dye-induced electrostatic potentials is that their increase with increased dye concentration is frequently much steeper (especially in negatively charged membranes) than those predicted by previous models based upon Gouy-Chapman diffuse double-layer theory, treating the electrostatic potential as arising from "smeared" charges (McLaughlin et al., 1971; McLaughlin and Harary, 1976; Andersen et al., 1978). This steepness could be explained by discrete charge effects (Andersen et al., 1978; Tsien, 1978). However, a couple of features of the data argue against a "discrete" charge effect as the sole explanation for the observed anomalies. The first is that for $diSC_1(5)$ and for $diSC_3(5)$ at 10^{-2} M ionic strength, the electrostatic potential behaviors as a function of dye concentration follow the Gouy equation; if low densities of adsorbed charges behaved as "discrete" charges, this effect should be observed regardless of the dye which is adsorbed (assuming that they sit at the same plane in the membrane). Secondly, the "discrete charge" models predict that the electrostatic potential vs. dye concentration behaviors should approach those predicted by the Gouy equation as the adsorbed charge density is increased, whereas no such effect is seen, despite the fact that for $diSC_5(5)$ in PE/PS the dye concentrations in the

membrane are at least as high as the highest seen in the fluorescence spectra of Fig. 13. In this latter case, membrane-bound monomer fluorescence was quenched in a manner which decreased with dilution of dye in the membrane phase. The most likely explanation for this phenomenon is Forster energy transfer which requires close proximity (i.e., less than or comparable to 100 Å separation; see, for example, Parker, 1968, pp. 83 ff.). In the bilayer experiments at high $diSC_5(5)$ concentrations, the dye molecules would be even closer than in the fluorescence experiments (as discussed in the Results), and considering their kinetic energy, they would long since have been expected to appear as "smeared charges" to a permeating ion. An alternative explanation for these anomalous electrostatic-potential behaviors in bilayers is that dye aggregates in the membrane phase are primarily responsible for the observed electrostatic potentials. The existence of such membrane-bound aggregates is supported by the dye spectral data.

Monactin-K^+ (or nonactin-K^+) was used as a "probe" to investigate whether an applied transmembrane potential causes a sufficient redistribution in the adsorbed dye species, either within the membrane phase or across the membrane-solution interface, to be detected as a voltage-dependent change in the membrane's apparent electrostatic potential. Although only small differences were observed in the conductance-voltage relationship induced by the "probes" in the presence and absence of the dyes, in the case of $diSC_8(5)$ it was clear that these differences were real, in that a time-dependent relaxation in the monactin-K^+-induced currents was observed in the presence, but not in the absence, of this dye. In the case of the other dyes, this same phenomenon may by occurring; if so, the relaxations are clearly no larger than for $diSC_8(5)$, and the time constants are fast enough that the relaxations are not observed by the present types of measurements.

The present results have some bearing on the usefulness of these dyes as monitors of transmembrane potentials and the mechanisms by which they might sense voltage changes. First of all, the spectral properties of the dyes are clearly sensitive to surface charge density as well as to transmembrane potential. Clearly any manipulation which alters the electrostatic surface potential produced by charges at, or near, the membrane surface (e.g. a change in concentration of charged, membrane-bound species or membrane constituents, or a change in screening of membrane surface charges) will alter the spectral signals observed for these dyes; thus, surface potential and transmembrane potential changes will be confounded. Such confounding is necessarily expected for any charged dye whose spectral properties are sensitive to the dielectric constant of its environment and which responds to voltage via redistribution either from one aqueous phase to the other or between the membrane and the aqueous phase. A corollary of this surface-potential effect is that different spectral signals will be observed for these dyes in response to the same change in transmembrane potential in membranes having different charge densities, and indeed such phenomena have previously been reported (Krasne, 1977). It would thus clearly be useful to be able to deduce the surface potential separately from the transmembrane potential.[3]

---

[3]A small confounding between surface potential and the electric field in the membrane could in principle be present in the experiments reported due to the asymmetry in distribution between PC and PS between the outer and inner halves of the bimolecular lipid leaflet in sonicated liposomes (Berden et al., 1975). Under the conditions of the present studies, approximately 20% more PS than PC is on the inner surface and the reverse on the outer surface. Although this might lead to an asymmetry in the distribution of dye and aggregates within these negatively charged

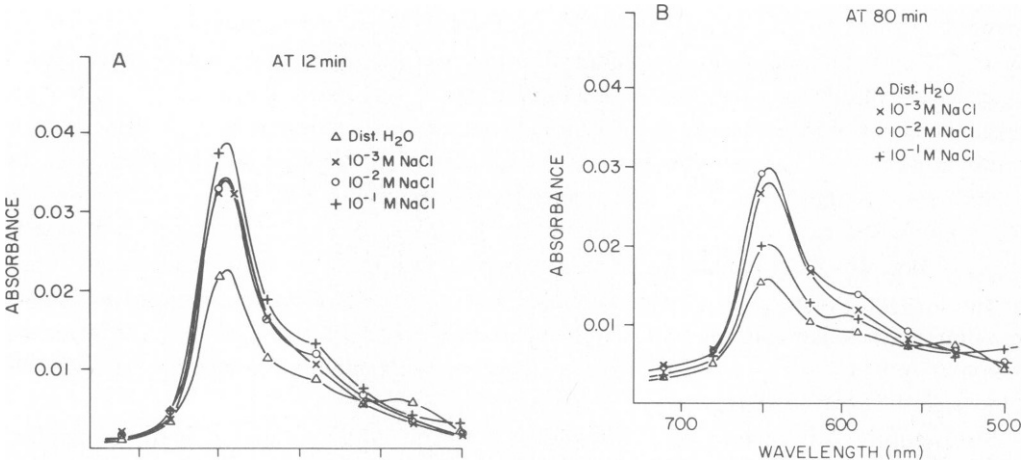

FIGURE 10 The time dependence of $diSC_2(5)$ absorbance as a function of aqueous ionic strength. The ordinate in each subfigure is absorbance and the abscissa is the wavelength. At time zero, $diSC_2(5)$ was added to 2×10^{-7} M in the sample cuvette, the spectra being recorded at 12 min (A) or 80 min (B) after dye addition. Spectra were scanned at 60 nm/min. The correspondence between the different symbols and aqueous compositions are indicated in the figure.

In addition, the data in this and the previous paper indicate that these dyes readily form membrane-bound aggregates. Under conditions (e.g. large negative surface-charge density) in which most of the dye is in the membrane phase, one might expect that the optical signal which one observes is governed primarily by a redistribution of dye and concomitant changes in dye aggregation within the membrane phase, whereas under conditions in which most of the dye is in the aqueous phase, this signal should reflect a change in the state of the dye in that phase. Since the state of aggregation of these dyes depends in turn upon the amounts of membrane phase and dye present in the system, the voltage response of dye fluorescence should also be dependent upon these variables (as has previously been found, Sims et al., 1974). Clearly these dyes monitor transmembrane potential changes by a "redistribution" mechanism. However, depending upon the variables cited above, the major redistribution may occur within the membrane, between the aqueous phases, or between the membrane and aqueous phases. Since the state of aggregation of the dye in each of these phases will also depend upon these variables, a large number of factors must be considered in any attempt to correlate a given change in dye spectrum with a given change in transmembrane potential.

APPENDIX

The purpose of this Appendix is to illustrate more fully the spectroscopic properties observed for the thiadicarbocyanine dyes. The influence of the aqueous ionic strength on the time dependence of the absorbance spectra for $diSC_2(5)$ is illustrated in Fig. 10. The spectra in Fig. 10 A were measured 12 min after adding 2×10^{-7} M $diSC_2(5)$ to either distilled water (Δ), 10^{-3} M(x), 10^{-2} M(o), or 10^{-1} M(+)

membranes, this factor would appear to contribute negligibly to the differences seen for these dyes between neutral and negatively charged liposomes since these same differences are observed (unpublished observations) between neutral and negatively charged, multilamellar, unsonicated liposomes (for which the lipids should be more uniformly distributed due to the larger radius of curvature; Berden et al., 1975).

NaCl solutions. Fig. 10 B illustrates the spectra measured for the same solutions 80 min after the addition of dye. Clearly the magnitude of the dye monomer peaks decreases with time; however the fractional decrease is not simply related to the ionic strength of the solution. At 90 min after dye addition, the aqueous solutions were removed and the dye adsorbed to the cuvette was solubilized in butanol. Correction for this adsorbed dye indicates that the actual dye concentrations in solution after 90 min had been 9×10^{-8} M, 1.6×10^{-7} M, 1.73×10^{-7} M, and 1.8×10^{-7} M for distilled H_2O, 10^{-3} M, 10^{-2} M, and 10^{-1} M NaCl solutions, respectively. Thus the decrease in the monomer peak is due in part to an ionic strength-dependent decrease in aqueous dye concentration with time due to glass adsorption, but at least in 10^{-1} M NaCl, it also reflects an increase in dye aggregation (creating an increase in absorbance at shorter and longer wavelengths) with time.

The absorbance spectra in Fig. 11 illustrate that the "apparent" extinction coefficient for the dimer peak increases whereas that for the monomer peak decreases in PC/PS liposomes with increasing concentration of $diSC_3(5)$. The ordinate is the absorbance divided by the dye concentration added to the aqueous phase; the broken curve illustrates the data for the aqueous dye spectrum in $diSC_3(5)$ just before the liposomes are added; and the solid curves are the spectra in the presence of liposomes for the dye concentrations indicated in the figure. The observed spectral behaviors provide additional confirmation that the peak observed at 595 nm in the presence of liposomes is due to a dye dimer in the membrane phase.

The absorbance spectra in Fig. 12 are those observed for $diSC_5(5)$. Subfigures A and B are for 10^{-3}M and 10^{-1} M NaCl + KCl (1:1), respectively, and additions of PC liposomes; subfigures C and D are for 10^{-3}M and 10^{-1}M NaCl + KCl (1:1), respectively, and additions of PC/PS. The broken lines are the spectra observed for the dye in the aqueous phase just before the first addition of liposomes and the solid lines and symbols are for the spectra observed for the dyes in the presence of liposomes at the concentrations of lipids indicated in the figure legend. The procedures employed to obtain these spectra

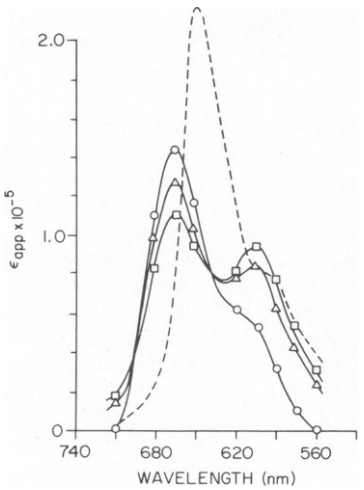

FIGURE 11 The formation of membrane-bound dimers by $diSC_2(5)$. The ordinate is the "apparent" extinction coefficient, ϵ_{app}, calculated by dividing the observed absorbance by the concentration to which the $diSC_2(5)$ was added, and the abscissa is the wavelength. The broken curve represents the extinction coefficients measured after adding $diSC_2(5)$ to a concentration of 1.3×10^{-7} M in 10^{-3} M KCl. The solid curves represent the extinction coefficients calculated from the absorbance spectra of 1.3×10^{-7} M (○), 4.5×10^{-7} M (Δ) and 7.7×10^{-7} M (□) $diSC_2(5)$ in the presence of 13 μg/ml PC/PS 4:1 (i.e. 80% PC, 20% PS) in 10^{-3} M KCl. Each spectrum was measured 5 min after the addition of dye and/or liposomes. Note that an increase in dye concentration causes a decrease in ϵ_{app} at 665 nm and an increase at 600 nm consistent with the behaviors expected if the former represents the absorbance maximum for the membrane-bound dimer.

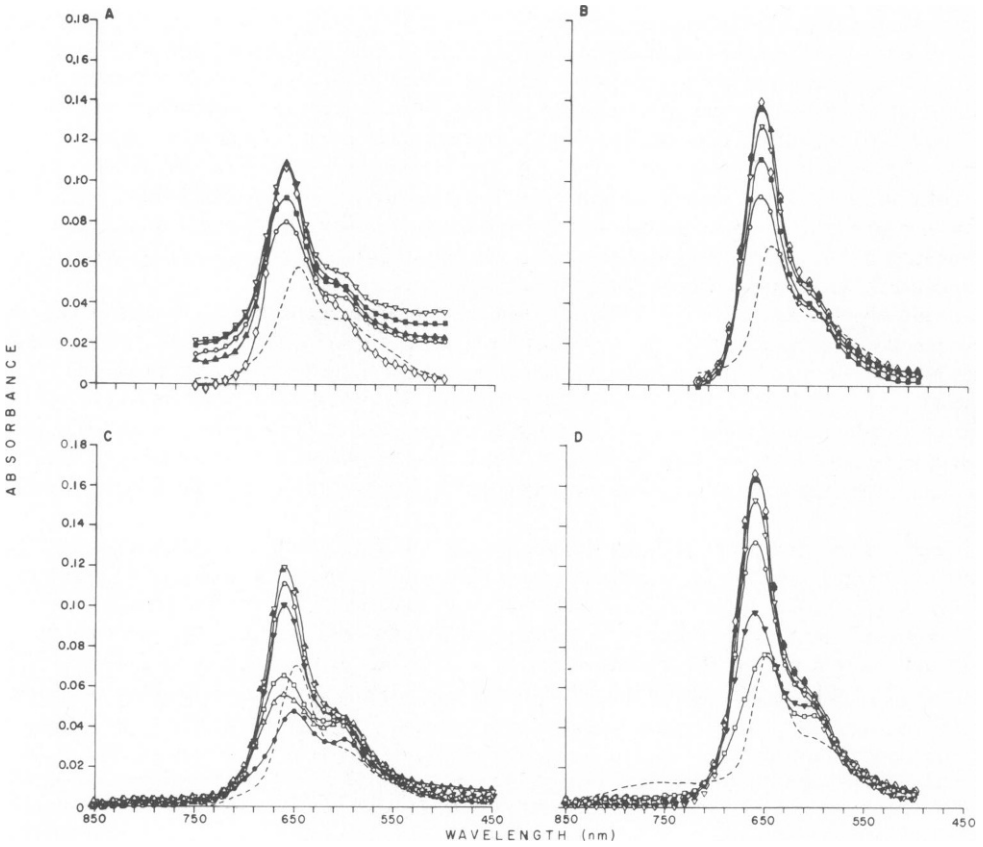

FIGURE 12 The influence of dye structure, membrane composition, and ionic strength on the absorbance spectra of $diSC_3(5)$. In each of these subfigures, the ordinate is absorbance, the abscissa is wavelength and $diSC_3(5)$ was added to a concentration of 10^{-6} M. The spectra in Figs. 12 and 13 were obtained as continuous curves, and the symbols have been inserted for purposes of identification. Subfigure A shows dye spectra for 10^{-3} M ionic strength and neutral, PC liposomes; sub figure B is for 10^{-1} M ionic strength and neutral PC liposomes; subfigure C is for 10^{-3} M ionic strength and negatively charged, PC/PS liposomes; and subfigure D is for 10^{-1} M ionic strength and negatively charged; PC/PS liposomes. The aqueous solutions consisted of 1:1 mixtures of KCl and NaCl, and internal solutions for the liposomes were always the same as external. The procedures for obtaining the spectra are described in the Methods of the text. In all subfigures, broken curves are spectra for the dye in the aqueous solution and the solid curves are spectra after additions of liposomes, the total concentration of lipid being indicated by a given symbol as follows: 0.148 μg/ml (●), 0.59 μg/ml (Δ), 1.48 μg/ml (□), 5.9 μg/ml (▾), 14.8 μg/ml (○), 29.6 μg/ml (■), 59.3 μg/ml (▿), 118.6 μg/ml (▲), 237.2 μg/ml (◇). The origins of the elevations in the spectra in Fig. 12 A at intermediate liposome concentrations are unknown; no increase in light scattering at 90° was observed to correlate with these elevations.

are discussed in the Methods, and the observations worthy of note are described in the body of this paper. Similar spectral measurements were made for the other dyes. For comparison, the fluorescence spectra for $diSC_3(5)$ are illustrated in Fig. 13 A–D. Since only the dye monomer is fluorescent, these spectra illustrate the distribution of dye monomer between the aqueous phase ($\lambda^{Fl}_{max} \simeq 665$ nm) and the membrane phase ($\lambda^{Fl}_{max} \simeq 680$ nm). Note that for high concentrations of dye monomer in the membrane phase, no fluorescence is observed even though absorbance peaks corresponding to dye monomer in the membrane are clearly present (e.g., cf. spectra for 0.59, 1.48, and 5.9 μg/ml PC/PS in 10^{-3} M ionic strength in Figs. 13 C and 12 C). In addition, the fluorescence peak for membrane-bound dye monomer

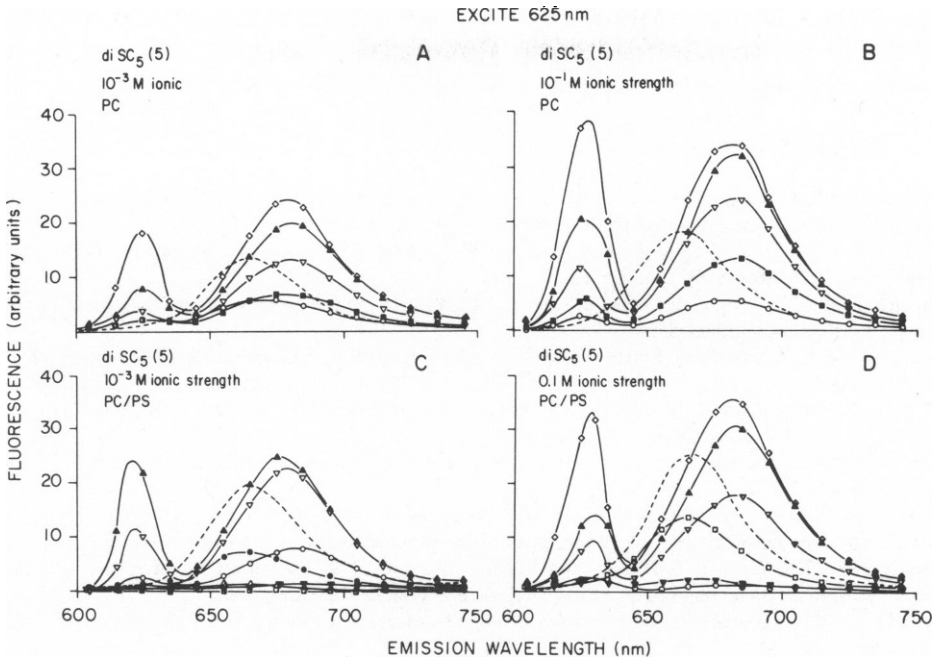

FIGURE 13 Fluorescence spectra for diSC$_5$(5) as a function of membrane composition and ionic strength. In each subfigure, the ordinate is fluorescence (in arbitrary units) and the abscissa is the emission wavelength. The excitation wavelength was 625 nm. The conditions for each subfigure are the same as those for the corresponding subfigure in Fig. 12, and the correspondence between symbols and lipid concentrations are also the same as for that figure. Each fluorescence spectrum was measured immediately following the corresponding absorbance spectrum in Fig. 12. The peak at 625 nm is due to light scattering from the liposomes, the peak at 665 nm (broken curve) corresponds to the fluorescence maximum for dye (monomer) in the aqueous phase, and the peaks at 680–685 nm correspond to the fluorescence maximum for dye (monomer) in the membrane phase. Note that the general behaviors of these spectra follow the behaviors of the dye monomer peaks in the corresponding absorbance spectra. Two important differences can be observed, however. One is that at high concentrations of dye in the membrane, the dye fluorescence is decreased to a much greater extent than that observed for dye monomer absorbance (cf., for example, the fluorescence and absorbance spectra for 5.9, 14.8, and 59.3 μg/ml lipid in Figs. 13 C and 12 C, respectively). Secondly, the dye fluorescence appears to increase, the wavelength maximum shifting to shorter wavelengths and the spectrum broadening to shorter wavelengths, with subsequent additions of liposomes at levels at which the corresponding absorbance spectra have virtually ceased to change with increasing liposome concentrations (cf., for example, fluorescence and absorbance spectra for 59.3, 118.6, and 237.2 μg/ml lipid in Figs. 13 D and 12 D, respectively). These two observations are evidence for energy transfer by these dyes in membranes as discussed in the text.

continues to increase with liposome additions long after the absorbance has reached a maximal value, and the fluorescence spectrum becomes broader on the side of shorter wavelengths. All of these behaviors are consistent with the hypothesis that the fluorescence due to monomers in the membrane phase is being "quenched" at high concentrations of membrane-bound dye by the process of energy transfer to nonfluorescent aggregates. This energy transfer may be an additional, important factor in quenching of fluorescence observed with increasing "hyperpolarizing" transmembrane potentials in liposomes and cells (cf. Sims et al., 1974; Hoffman and Laris, 1974).

I am most grateful to A. Waggoner, C-H. Wang, and J. Smith for providing me with the dyes discussed in this and the previous paper and to S. Ciani and S. McLaughlin for many helpful suggestions and discussions throughout the

course of this work. The research reported here and in the previous paper was supported by National Institutes of Health grant HL 20254.

Received for publication 29 May 1979 and in revised form 24 January 1980.

REFERENCES

ANDERSEN, O., S. FELDBERG, H. NAKADOMARI, S. LEVY, and S. MCLAUGHLIN. 1978. Electrostatic interactions among hydrophobic ions in lipid bilayer membranes. *Biophys. J.* **21**:35–70.

BANGHAM, A. D., M. W. HILL, and N. G. A. MILLER. 1974. Preparation and use of liposomes as models of biological membranes. *Meth. Membrane Biol.* **1**:1–68.

BASHFORD, L. C., B. CHANCE, J. C. SMITH, and T. YOSHIDA. 1979. The behavior of oxonol dyes in phospholipid dispersions. *Biophys. J.* **25**:63–85.

BATZRI, S., and E. KORN. 1973. Single bilayer liposomes prepared without sonication. *Biochim. Biophys. Acta.* **298**:1015–1019.

BERDEN, J., R. BARKER, and G. RADDA. 1975. NMR studies on phospholipid bilayers: some factors affecting lipid distribution. *Biochim. Biophys. Acta.* **375**:186–208.

COHEN, L., and B. SALZBERG. 1978. Optical measurement of membrane potential. *Rev. Physiol. Biochem. Pharmacol.* **83**:35–88.

COHEN, L., B. SALZBERG, H. DAVILA, W. ROSS, D. LANDOWNE, A. WAGGONER, and C-H. WANG. 1974. Changes in axon fluorescence during activity: membrane probes of membrane potential. *J. Membr. Biol.* **19**:1–38

EISENBERG, M., T. GRESALFI, T. RICCIO, and S. MCLAUGHLIN. 1979. The adsorption of monovalent cations to bilayer membranes containing negative phospholipids. *Biochemistry.* **23**:5213–5223.

HENRY, D. C. 1938. A source of error in micro-cataphoretic measurements with a cylindrical-bore cell. *J. Chem. Soc. (Lond.)* 997–999.

HLADKY, S., and T. RINK. 1976. Potential difference and the distribution of ions across the human red blood cell membrane: a study of the mechanism by which the fluorescent cation, diS-C_3-(5) reports membrane potential. *J. Physiol. (Lond.)* **263**:287–319.

HOFFMAN, J., and LARIS. 1974. Determination of membrane potentials in human and amphiuma red blood cells using a fluorescent probe. *J. Physiol. (Lond.).* **239**:519–552.

KAY, R., E. WALWICK, and C. GIFFORD. 1964. Spectral changes in a cationic dye due to interaction with macromolecules. I. Behavior of dye alone in solution and the effect of added macromolecules. *J. Phys. Chem.* **68**:1896–1916.

KLEIN, R. A. 1970. The detection of oxidation in liposome preparations. *Biochim. Biophys. Acta.* **210**:486–489.

KRASNE, S. 1977. Cyanine dye-induced electrical and fluorescence effects in neutral and negative bilayer membranes. *Biophys. J.* **17**:214*a*. (Abstr.)

KRASNE, S. 1980. Interactions of voltage-sensing dyes with membranes. I. Steady-state permeability behaviors induced by cyanine dyes. *Biophys. J.* **30**:000–000.

MCLAUGHLIN, S. 1977. Electrostatic potentials at membrane-solution interfaces. *Curr. Top. Membranes Transp.* **9**:71–144.

MCLAUGHLIN, S., and H. HARARY. 1976. The hydrophobic adsorption of charged molecules to bilayer membranes: a test of the applicability of the Stern equation. *Biochemistry.* **15**:1941–1948.

MCLAUGHLIN, S., G. SZABO, and G. EISENMAN. 1971. Divalent ions and the surface potential of charged phospholipid membranes. *J. Gen. Physiol.* **58**:667–687.

PARKER, C. A. 1968. *Photoluminescence of Solutions.* Elsevier Scientific Publishing Co., Amsterdam. pp. 83 ff.

SIMS, P., A. WAGGONER, C. WANG, and J. HOFFMAN. 1974. Studies on the mechanism by which cyanine dyes measure membrane potential in red blood cells and phosphatidylcholine vesicles. *Biochemistry.* **13**:3315–3329.

SZABO, G., G. EISENMAN, S. MCLAUGHLIN, and S. KRASNE. 1972. Ionic probes of membrane structures. *Ann. N.Y. Acad. Sci.* **195**:273–290.

WAGGONER, A. 1976. Optical probes of membrane potential. *J. Membr. Biol.* **27**:317–334.

WAGGONER, A., C. WANG, and R. TOLLES. 1977. Mechanism of potential-dependent light absorption changes of lipid bilayer membranes in the presence of cyanine and oxonol dyes. *J. Membr. Biol.* **33**:109–140.

WEST, W., and S. PEARCE. 1965. The dimeric state of cyanine dyes. *J. Phys. Chem.* **69**:1894–1903.